OVERSHOOTING CLOUD TOP DETECTIONS USING MSG SEVIRI INFRARED BRIGHTNESS TEMPERATURES AND THEIR RELATIONSHIP TO SEVERE WEATHER OVER EUROPE

Kristopher M. Bedka

Science Systems and Applications Incorporated, Hampton, VA

Corresponding Author Address: Kristopher M. Bedka

Science Systems and Applications, Inc.

1 Enterprise Parkway, Suite 201

Hampton, VA 23666 USA

Email: Kristopher.m.bedka@nasa.gov

Phone: (757) 951-1920

Fax: (757) 951-1902

Keywords: Deep convection, satellite, Meteosat-8/9, SEVIRI, overshooting convective cloud tops, severe weather, European Severe Weather Database

ABSTRACT

This purposes of this paper are to: 1) demonstrate an objective overshooting top (OT) detection method using Meteosat Second Generation (MSG) Spinning Enhanced Visible and Infrared Imager (SEVIRI) infrared data, 2) produce an OT database for all operational SEVIRI data over Europe and north Africa for the six Northern Hemisphere warm seasons observed by SEVIRI to date, and 3) determine the frequency of OT detections in the vicinity of confirmed severe weather reports recorded within the European Severe Weather Database (ESWD). Algorithm performance is demonstrated for a case where numerous severe storms were present. Qualitative comparisons indicate that most OT detections correspond with the characteristic OT signature in SEVIRI 1 km resolution visible channel imagery, but some OTs were left undetected due in part to relatively coarse SEVIRI spatial resolution over the European domain.

The SEVIRI OT database shows a strong relationship between OT maxima and regions with high terrain. OTs are found to occur more frequently during the day over land and during the night over water. Inter- and intra-seasonal variability in OT frequency and location are also shown. An OT was found near 47% of the confirmed ESWD events. The OT-severe weather relationship is strong for large hail (53%) and severe wind (52%) events but relatively weak for tornado events (14%). The weak OT-tornado relationship may be related two factors: 1) low-level wind shear is found to be of greater importance than large CAPE and strong updrafts (i.e. OTs) in tornadic storm environments across Europe and 2) a weakening of the storm updraft and collapse of the OT region has been documented prior to tornado formation. The relatively strong overall OT-severe weather relationship suggests that OT detections can be used to

increase forecaster confidence that a given storm is severe, especially in regions where frequent, ground based Doppler weather radar data is unavailable.

1. Introduction

Overshooting tops (OTs) are the product of deep convective storm updraft cores of sufficient strength to rise above the storms' general equilibrium level in the tropopause region and penetrate into the lower stratosphere. Thunderstorms with OTs frequently produce hazardous weather at the Earth's surface such as heavy rainfall, damaging winds, large hail, and tornadoes. (Reynolds 1980; Negri and Adler 1981; Adler et al. 1985; Brunner et al. 2007). Turbulence and cloud-to-ground (CG) lightning are found to occur most frequently near the OT region, indicating that OTs represent significant hazards to ground-based and in-flight aviation operations (Machado et al. 2009; Bedka et al. 2010). Safer aviation operations can be achieved if the locations of these areas are known in a timely manner.

Bedka et al. (2010) describes a new method for objective OT detection using a combination of 11 μm infrared window (IRW) channel brightness temperatures (BTs), a numerical weather prediction (NWP) model tropopause temperature forecast, and OT size and BT criteria defined through analysis of 450 thunderstorm events within 1-km Moderate Resolution Imaging Spectroradiometer (MODIS) and Advanced Very High Resolution Radiometer (AVHRR) imagery. This method is called "IRW-texture" because it utilizes BT spatial gradients (i.e. texture) to identify clusters of pixels that are significantly colder than the surrounding anvil cloud and have a size consistent with commonly observed OTs. They demonstrated the IRW-texture method using the Twelfth Geostationary Operational Environmental Satellite (GOES-12), MODIS, and synthetic GOES-R Advanced Baseline Imager (ABI, Schmit et al. 2005) data.

The technique is dependent on the imager resolution. For example, Bedka et al.

(2010) found that the number of detected OTs decreases from 17 to 3 when 1 km MODIS is replaced with 4 km GOES-12 imagery for one event over the continental U.S.. Despite this resolution dependence, Bedka et al. (2010) show that the IRW-texture outperforms an existing, well-documented OT detection method based on the 6 to 7 μm water vapor (WV) absorption minus the ~11 μm IRW channel BT difference (WV-IRW BTD) with numerous qualitative and quantitative examples.

Applying the method to 5 years of warm-season (April-September) GOES-12 data taken over the eastern two-thirds of the U.S., Bedka et al. (2010) found some very interesting geographic and diurnal variability in OT activity. The Rocky Mountain and Southeast U.S. regions exhibited strong daytime OT maxima, portions of the U.S. Great Plains exhibited a nighttime OT maximum, and the region coinciding with the position of the Gulf Stream ocean current featured frequent OTs during both day and night.

There have been very few climatological studies of European deep convection from a satellite perspective. Considerable effort has been directed toward identifying the environments favorable for and locations of severe thunderstorms over Europe. Brooks et al. (2003) analyzed global reanalysis datasets to determine the global spatial distribution of environments favorable for severe thunderstorms. They determined that, on average, the air mass over Europe is not as favorable for severe storms as that present over much of the United States. The European environment features smaller mid-level lapse rates and a much drier boundary layer (in terms of water vapor mixing ratio) which combine to reduce the mean Convective Available Potential Energy (CAPE). Databases of severe storms producing hail, damaging winds, and/or tornadoes have first been developed for individual European countries: Czech Republic

(Setvak et al. 2003), Finland (Tuovinen et al. 2009), Germany (Dotzek 2001; Bissolli et al. 2007), Greece (Sioutas 2003), Great Britain and Ireland (Webb et al. 2009), Hungary (Horvath 2003), Italy (Giaiotti 2007), and Spain (Sanchez et al. 2003). These combined local spotter or media reports and ground-based weather radar observations. Since 2006, the European Severe Storms Laboratory (ESSL) has been collecting and quality-controlling such reports in the European Severe Weather Database (ESWD, Groenemeijer et al. 2004; Dotzek et al. 2009), which can be used to determine regions most often impacted by severe storms.

Morel and Sénési (2002) describe perhaps the most comprehensive satellite-based European convective cloud climatology to date. They describe an automated method for mesoscale convective system (MCS) identification and tracking using Meteosat IRW imagery over Europe, the Mediterranean, and north Africa during the warm season (April-September). In their study, an MCS is defined by a ≥ 1000 km^2 area of adjacent pixels with IRW BT ≤ 228 K (-45° C). They found that European MCSs are mainly continental, but MCSs become more frequent over the Mediterranean Sea during the latter part of the warm season. The location of first detection of European MCSs (i.e. triggering) is strongly correlated with orography and relative maxima of MCS triggering are observed near all mountain ranges. They also describe the variability in location of MCS occurrences throughout the warm season.

It is important to determine regions where OTs most often occur around the world as they have been shown to be an aviation weather hazard and are often observed in satellite imagery near confirmed severe weather events. Additionally, OTs can inject water vapor into the stratosphere which is important because water vapor is a major

greenhouse gas. Though Morel and Sénési (2002) document the occurrence of large storm complexes over Europe, an OT occupies only a small fraction of the convective anvil cloud (Bedka and Minnis 2010) and OTs can occur within storms far smaller than their ≥ 1000 km^2 MCS minimum area criterion.

The purpose of this paper is to demonstrate the IRW-texture OT detection capability using data from the Meteosat Second Generation (MSG) Spinning Enhanced Visible and Infrared Imager (SEVIRI) instrument aboard the Meteosat-8 and -9 satellites. An OT database, similar to that described by Bedka et al. (2010) over the U.S, is produced for Europe and North Africa using SEVIRI IRW data from April-September 2004-2009. This time period, albeit too short to serve as a climatology, covers every Northern Hemisphere warm season observed by the SEVIRI instrument to date. OT detections from this database are compared with damaging wind, large hail, and tornado reports from the ESWD to investigate the potential for using OT detections to identify severe storms.

2. Data

2.1 Satellite Imagery

MSG SEVIRI 10.8 μm IRW channel imagery is used as the primary input to the IRW-texture OT detection algorithm. All 15-minute resolution 10.8 μm (SEVIRI channel 9) BT data from April-September 2004-2009 are processed. The domain of interest in this study covers a region from 30° to 60° N and 10° W to 30° E (see Figure 1). Table 1 shows the pixel sampling distance in the southwest corner, center, and northeast corners of the domain, illustrating marked sampling differences in the scan line direction

which can have significant impact on IRW-texture OT detection capability. SEVIRI data from Meteosat-8 was used from April 2004 to early April 2007. SEVIRI data from Meteosat-9 was used from April 2007 through September 2009. The SEVIRI data were provided by the University of Wisconsin Space Science and Engineering Center (UW-SSEC) Data Center.

2.2 Numerical Weather Prediction Tropopause Temperature

A 6-hour forecast of tropopause temperature from the one-degree resolution Global Forecast System (GFS) NWP model is also used as input to the IRW-texture OT detection algorithm. The 6-hr forecast is used to emulate the processing method and performance that would occur if the algorithm were run in real time. This NWP field is remapped to the resolution and projection of the corresponding satellite imagery using the Man Computer Interactive Data Access System (McIDAS) software package (Lazzara et al. 1999) so that a tropopause temperature is associated with every satellite pixel.

2.3 European Severe Weather Database

ESWD reports (http://www.eswd.eu) were provided by the European Severe Storms Laboratory for use in this study. The main objective of the ESWD is to collect and provide detailed, quality-controlled information on severe convective storm events over Europe using a homogeneous, interoperable data format with a web-based user-interface where both the collaborating national meteorological and hydrological services (NMHS), spotter organizations, and the public can contribute and retrieve observations.

These features were necessary to overcome the previous fragmentation of severe weather databases in Europe, and to gain acceptance by the European NMHS.

Reports of severe wind, large hail, and tornadoes were extracted from the ESWD during the April-September 2004-2009 period within the study domain described above. The ESWD distinguishes four quality-control (QC) levels (Dotzek et al. 2009): QC0 "as received", QC0+ "plausibility checked", QC1 "report confirmed by reliable sources", and QC2 "event fully verified". ESWD quality-control levels denote the reliability of the contained information, and do not refer to the mere quantity of information (number of filled database fields). The significant step in report quality takes place from QC0+ to QC1. Both QC1 and QC2 reports are confirmed and suitable for quantitative analysis. However, for some analyses, even the QC0+ reports will still be adequate.

Severe storm reports that have been confirmed (QC1) or fully verified (QC2) by either the ESSL or NMHS are used here. A total of 1475 severe storm reports meet these criteria and are compared with OT detections using the methodology outlined below. It is important to note that severe winds recorded in the ESWD can be produced by non-convective events. To identify these cases, the ESWD contains a special data field, similar as for cases in which the wind damage might have been caused by a tornado. This has not been taken into account in our study and can affect (i.e. reduce) any statistical relationship between severe winds and OTs derived using the methodology described below.

2.4 Surface Elevation Dataset

The “ETOPO1” dataset is a 1 arc-minute global relief model of Earth's surface

that integrates land topography and ocean bathymetry. The best available digital data from diverse global and regional digital data sets were obtained, shifted to common horizontal and vertical datums, and evaluated and edited before digital elevation model generation, Amante and Eakins 2009). The ETOPO1 dataset from the U.S. National Geophysical Data Center is used to provide a detailed depiction of the land surface elevation over the study domain in addition to an objective differentiation between land and water surfaces. Locations with sub-zero elevation were classified as water in this study. This designation will be used to determine differences in OT frequency over land and water surfaces throughout the day.

3. Methodology

3.1 IRW-texture OT Detection

Bedka et al. (2010) describe the IRW-texture OT detection algorithm in full detail, but a short summary is provided here for context. The algorithm is formulated around the premise that OTs appear as small clusters of pixels (≤ 15 km diameter) that are significantly colder than the surrounding anvil cloud. Relative BT minima that are lower than 215 K are first identified. These pixels are then compared to an NWP tropopause temperature to verify that these pixels are indeed cloud tops "overshooting" their equilibrium levels in the tropopause region. Due to the relatively coarse resolution of the geostationary data used here, most notably in the northeast portions of this domain, the very low IRW BTs within OTs often observed in higher resolution polar-orbiting imager data cannot be detected. Thus, a significant number of pixels across this domain, especially those associated with weak OTs, would never be considered if all

pixels were required to be colder than the NWP tropopause. In an attempt to mitigate this issue, pixels will progress into subsequent stages of processing if they are no more than 2.5 K warmer than the NWP tropopause.

Checks are then performed to ensure that no minima are located within 15 km of each other so that portions of the same OT are not classified as two independent tops. The IRW BT of the anvil cloud surrounding the potential OT is then sampled at an ~8 km radius in 16 directions. The surrounding anvil pixels must have an IRW temperature at or colder than 225 K to be included in the mean computation. At least 5 valid anvil pixels must be present. The 5-of-16 pixel criterion is imposed to ensure that the anvil is of relatively large horizontal extent but allows an anvil to occupy as small as a 90° quadrant which might be the case when strong jet-level winds are present. A pixel is classified as an overshooting top if it is ≥ 6.5 K colder than the mean BT of the surrounding anvil cloud. This would imply that the pixel is 0.7 to 0.9 km above the anvil (Adler et al. 1983). As this process identifies only one pixel at the location of an OT minimum BT, a filling procedure is performed when necessary to capture the remaining neighboring pixels that comprise the entire OT.

Using a combination of synthetic satellite imagery and cloud top height derived from a cloud-resolving NWP simulation, Bedka et al. (2010) show that both a greater OT-anvil BT difference and a greater number of pixels included in the mean can be used to reduce the false alarm ratio (FAR) of OT detections. Their results show a FAR ranging from 4.2 to 38.8% depending on the values of these two parameters and the magnitude of overshooting considered.

For this study, only the single pixel located at the OT IRW BT minimum is recorded. The OT detections are corrected for parallax based on a cloud-top height of 14 km to better match their actual positions relative to the Earth surface. It is well understood that the peak OT height is not constant across all events, so there will be some small error in parallax correction if the peak height differs significantly from 14 km. For example, at a coordinate of 45° N, 10° E, a peak height of 15 km would require an additional 1.3 km correction, which is relatively insignificant to the results in this paper. The results are grouped into 0.5° bins to better depict the regions with the most frequent OT activity. Detection results are separated into daytime (9:00 AM to 8:45 PM LST) and night-time (9:00 PM to 8:45 AM) periods to investigate diurnal patterns in OT activity throughout the domain. Results are grouped into 1.5° x 1.5° boxes to achieve a significant OT sample size to evaluate OT diurnal trends. Detection results are also grouped into hourly bins to determine periods when OTs are most frequent over both land and water. For example, a data point at 1500 UTC represents a summation of all OT detections from the four SEVIRI scans (assuming all four are present at the UW-SSEC Data Center) during the 1500-1545 UTC time period. Detections are also grouped by month and year to show intra-seasonal variability of OT activity.

3.2 Comparison between the ESWD and OT Detections

The objective of the comparison between the ESWD and OT detections is to determine how often OTs are detected near the time and location of confirmed severe weather reports. If this frequency were relatively high, then OT detection output could be used as an additional parameter to increase forecaster confidence that a given storm

is producing severe weather, especially in regions where frequent, ground-based Doppler weather radar data is unavailable. It is well understood that there is still underreporting of severe weather events in a number of regions in Europe (see Dotzek et al., 2009; Groenemeijer et al., 2009). Therefore we cannot answer the reverse and ultimately more useful question, namely, how often could one expect severe weather to occur near any detected OT?

A variable time and distance window is used when matching OTs with severe weather events based upon the specified confidence of time of the severe event within the ESWD. For some reports, the exact time of that the event occurred is very well known and a confidence interval of +/- 1 minute is assigned to the report. For others, the confidence is very low and the interval can be as large as +/- 1 day. Severe events with a confidence ≤ +/- 1 hour are used in this study.

The SEVIRI image time stamp represents the time at which the first scan line is recorded. SEVIRI begins its scanning in the Southern Hemisphere and takes approximately 10 mins to collect data over Europe. The SEVIRI time stamp is increased by 10 mins in this study to account for the scan delay. For a confidence ≤ +/- 15 mins, any OT detection from a SEVIRI image within this 30 min time window is considered a match with an ESWD report if it is within 25 km of the report location. This distance criterion takes into account 1) a maximum storm motion of 60 km/hr, 2) possible error in parallax correction for OTs with heights that differ from 14 km, and 3) possible error in the reported latitude/longitude of the severe storm event. For a confidence of +/- 1 hour, a 75 km distance match criterion is used.

4. Results

4.1 Demonstration of Overshooting Top Detections Using MSG SEVIRI

IRW-texture OT detections from an individual event will be discussed first to demonstrate the performance of this algorithm with MSG SEVIRI data. The event of interest occurred on 25 May 2009, when 24 confirmed severe storm reports were recorded within the ESWD across this domain (Figure 2). Satellite imagery and derived products for this event are being studied in detail by the Convection Working Group (CWG), convened by EUMETSAT and the ESSL (http://convection.satreponline.org/about.php). The focus of the CWG is to develop a comprehensive inventory of the available convective storm diagnosis and nowcasting techniques/products with the aim of getting a deeper insight into their differences, commonalities, and specific areas of application.

Hourly SEVIRI IRW imagery from 1000-1700 UTC shows an intense, long-lived hailstorm that moved across northern France, Belgium, and western Germany throughout this time period (Figure 3). Numerous other storms propagated into this domain or initiated on and after 1300 UTC, including a storm cluster along the English Channel and a severe storm in the Austria-Slovenia border region, both of which will be discussed in detail below.

IRW-texture OT detections are shown for all 15-minute SEVIRI scans during the 1000-1659 UTC time period (Figure 4). Based on a comparison of the ESWD with OT detections for this case, all severe storms were associated with an OT detection, though not every storm with an OT was near a severe storm report. A cluster of OT detections are found during the 1000-1230 UTC time frame along the France-Belgium border

region, coincident with many large hail reports. The OT detection field does not continue in this linear pattern after 1300 UTC, even though large hail continues to be reported across eastern Belgium and western Germany until 1330 UTC. A close examination of the IRW BT imagery after 1230 UTC shows a U-shaped pattern, but reveals few time periods when a distinct minima in the BT field is present (not shown). Setvak et al. (2010) have noted the lack of distinct BT minima at the apex of a U-pattern or within the ring pattern for storms across central Europe, though significant minima are common for U-shaped storms over the U.S. observed in 1 km AVHRR and MODIS imagery (Brunner et al. 2007). OTs without a distinct BT minimum cannot be detected by the IRW-texture method (Bedka et al 2010).

Figures 5 and 6 show IRW-texture OT detections and the corresponding SEVIRI imagery in detail for storms present over northern France and the English Channel and the Austria-Slovenia border region, respectively. These storms were selected for detailed analysis because they occurred during the late afternoon when the solar zenith angle is large and OTs are better depicted in 1 km SEVIRI High Resolution Visible (HRV) channel imagery. For the English Channel event, OTs are consistently detected within storm “B” and comparison of these detections with the characteristic “lumpy” OT signature in HRV imagery would suggest that many of them are accurate detections.

The OT region identified by the arrow within storm “A” was detected in only one (1500 UTC) of the four images. A distinct BT minimum was present at the time of the detection in conjunction with the emergence of the cold ring signature. At 1530 and 1600 UTC, the OT signature was still apparent in HRV imagery as the central warm spot became prominent, but there was very little evidence of a BT minimum in the OT

region. Setvak et al. (2010) analyzed IRW BT patterns in cloud-resolving model output for a storm with a cold ring and U/V signature. They suggest that air parcels within a long-lived OT mix with the ambient stratospheric environment, causing the OT to warm with time. Though it would be unusual for a single OT to persist for longer than an hour, we might be observing this warming if the same OT were present in storm A across the image sequence. It is difficult to definitively prove this with the currently available 5 to 15 minute SEVIRI imagery because one OT can collapse and be replaced by another due to pulses in the storm updraft that could occur in the time between images. Future generation sensors such as the GOES-R ABI will provide 30 second imagery over regional domains for high impact events which will help us to better observe and understand this process.

The WV-IRW BTD is also insignificant in the OT region relative to surrounding values within storm “A” (Figure 6). Thus no existing infrared-based detection technique could detect this OT. Furthermore, the WV-IRW BTD technique would produce substantial false alarm for both storms regardless of the selected BTD detection criteria, a problem noted by Bedka et al. (2010).

The discussion is now directed toward a more “typical” case where OTs are present in scattered convection along the Austria-Slovenia border region (Figure 7). Severe weather was not reported with many of these storms, though the storm shown at the center of the domain at 1630 UTC did produce large hail and heavy rain as it moved southward into Slovenia. OTs are identified at all times within this sequence, including those clearly evident in the southernmost storm of this cluster. Comparison to HRV imagery suggests that many of the detections are accurate, though it is clear that some

likely OTs also went undetected. Maxima in the WV-IRW BTD were often present in locations of IRW-texture OT detections, but false alarm also occurred again in non-overshooting convective anvil clouds (Figure 8).

It has been shown here that the IRW-texture technique cannot detect every OT that may be present within a given set of storms due to factors such as limited IRW channel spatial resolution and inconsistency between OT signatures in visible channel imagery and the corresponding IRW BT field. Nevertheless, the above results coupled with those of Bedka et al. (2010) suggest that this technique produces reliable output with fewer false alarms than other available infrared-based day/night detection methods and would be applicable for producing a representative OT climatology using SEVIRI data. The remainder of the paper will focus on description of the SEVIRI 2004-2009 warm season OT database results.

4.2 MSG SEVIRI Overshooting Top Database

Gridded OT detection frequency is shown in Figure 9 over the study domain. The OT maxima are well correlated with regions of high terrain (Figure 1), which agrees well with the favored locations of MCS triggering described by Morel and Sénési (2002). A total of 62,032 OTs were detected during the six warm seasons analyzed in this study, equating to ~57 per day on average. The region with the most frequently detected OTs is located along the Austria-Italy border (Latitude: 46.5° N, Longitude: 13° E) where 88 OTs were detected within +/- 0.25° of this point, equating to ~1 OT every ~12 warm season days on average. The location of this OT maximum agrees quite well with a regional maximum in CG lightning activity during 1992-2001 described by Schulz et al.

(2005). The number of OTs in this region is far fewer than the 200+ detections over the southeast U.S. shown by Bedka et al. (2010). As Brooks et al. (2003) have pointed out, the mean CAPE over the U.S. is larger than that over Europe which would yield stronger storm updrafts and perhaps OTs that are more prominent and easier to detect than those over Europe, despite the coarser GOES-12 spatial resolution.

OTs were more frequently detected over land during the daytime (0900 AM to 0845 PM local time (LT), Figure 9b) and over the water during the night-time (0900 PM – 0845 AM LT, Figure 9c). The strong daytime bias is most pronounced across Eastern Europe, Spain, and in regions of high elevation (Figure 9d). This daytime OT bias for high elevation regions agrees with the results over the U.S. Rocky Mountains shown by Bedka et al. (2010). The OT bias is neutral and in some cases shifted to a night-time bias over western France, the Low Countries, northern Germany and Poland, and in the Baltic States where maritime climates are prevalent. This nighttime OT bias over water also agrees with the results over the Atlantic Ocean of Bedka et al. (2010).

OT activity maximizes during the afternoon and early evening over land, peaking at 5 PM LT in association with the time period of highest land surface temperatures and greatest atmospheric instability (Figure 10). The pattern in OT activity over water is a bit more complex with a general increase occurring between 12 and 11 PM LT and a distinct maximum in the early morning (05-07 AM LT). The broad maximum over water in the latter third of the 12-11 PM interval coincides with a significant OT decrease over land, suggesting that this may caused by a combination of 1) storms that initially develop over land but drift over nearby bodies of water, 2) land/sea breeze circulations that initiate storms over coastal waters, and 4) storms forced by mid-latitude cyclones

that do not require solar heating to maintain storm intensity due to warm sea surface and abundant boundary layer moisture. OTs detected during the secondary 05-07 AM maximum were concentrated in the western half of the Mediterranean Sea and along the northern and eastern shores of the Adriatic Sea (Figure 11). This result agrees with the CG lightning maximum in the 06-07 AM timeframe over the western Mediterranean identified by Rivas Soriano and de Pablo (2002). Monthly OT suggest that the western Mediterranean OTs occur primarily in May and August-September in association with increased mid-latitude cyclone activity across this region (see Figure 13b,e-f, to be described later), but OTs over water in other regions were more equally distributed throughout the warm season.

Interannual variations in detected OTs are significant, hence our short-term climatologic results must be interpreted with caution. A substantial number of OTs occurred during 2004, followed by a significant decrease within the 2005-2006 period, and then a steady increase in activity year over year from 2007-2009 (Figure 12). The relative minimum during 2005-2006 coincides with drought conditions that occurred during these two warm seasons across much of Europe (http://www.eumetsat.int/Home/Main/News/CorporateNews/005280?l=en). The results also indicate that 2008 and 2009 were especially active across the Mediterranean Sea.

When OT detections are separated by month (Figure 13), the results show a widely dispersed but relatively small number of OTs in April as the land surface is still quite cool and boundary layer moisture is limited. OT activity rapidly increases in May and reaches a peak in June across continental Europe. OT activity then decreases in July and August, especially over the Iberian Peninsula and northern Africa, as a sub-

tropical high pressure expands over the domain and acts to suppress convective storm activity. This is followed by a significant OT increase over the Mediterranean region during September in association with a sharp increase in mid-latitude cyclone activity, especially during 2008-2009 as shown above, and a decrease across continental Europe likely as a result of an increasing sun angle and cooling land mass.

4.3 Overshooting Top and European Severe Weather Database Comparison

Though a qualitative comparison of Figures 2 and 4 may suggest a relationship between OT detections and storm severity for an individual case, it is important to determine a quantitative relationship with a large sample size of events to increase forecaster confidence that severe weather could be occurring in close proximity to an OT. Using the methodology described above, an OT was found in the vicinity of severe weather events for 687 or ~44% of the 1475 confirmed reports (Table 2). The relationship is strongest for large hail events (53%) and weakest for tornado events (14%). The relationship is also relatively strong for severe wind events (52%).

A storm with a well-defined OT indicates the presence of a strong updraft that extends through the equilibrium level. In general, significant atmospheric instability, quantified through bulk parameters such as CAPE or Lifted Index, is required to produce such an updraft. Large hail is strongly correlated with steep lapse rates and high CAPE values throughout the mid level of the storm. These are necessary to produce strong updrafts that prevent hailstones from falling down to the ground before they have reached considerable diameters. Severe wind gusts in association with OTs can be produced by downward transfer of high momentum air from aloft and by

downdrafts induced by evaporative cooling or melting of small hail in the region surrounding the OT (e.g., Dotzek and Friedrich, 2009).

There is evidence that suggests that strong wind shear is found more often than high CAPE in tornadic thunderstorm environments across Europe. For instance, Groenemeijer and van Delden (2007) have shown in one particular study over the Netherlands that the mean "most unstable" CAPE (MUCAPE) is 1072 J kg^{-1} for severe hail producing storms. The mean MUCAPE for tornadic storms was ~400 J kg^{-1}, yielding a much weaker updraft than that present within hail storms. Sander et al. (2008), Brooks (2009), and Kaltenböck et al. (2009) found that severe storms in an environment with large 0–1 km wind shear and a low lifted condensation level are most likely to produce a significant tornado across Europe. Large CAPE was of secondary importance to these two parameters. In low CAPE environments, OTs may not be as pronounced in IRW BT imagery or possibly not present at all, thereby contributing to the weak OT-tornado relationship.

However, tornadoes over Europe do also form in high CAPE environments in some cases, so we offer another hypothesis that may also contribute to the low frequency of OT detections near tornadoes. Several studies have indicated updraft weakening and collapse of the OT prior to the formation of a tornado (Lemon et al. 1978; Adler and Fenn 1981; Steiger et al. 2007). Of the ESWD tornado observations included in this study, 63% (218 of 345) have a temporal confidence at or better than +/- 15 mins. An OT was detected for 24 of these 218 events, but only 2 of 24 OTs were detected prior to the time of the tornado. This supports the OT collapse hypothesis, though the results are considered inconclusive because of the small sample size. Due

to the weak IRW-texture OT-tornadic storm relationship shown in this study, objective detection of tornadic storms across Europe using IR imagery may require an alternative approach.

The relationships for the large hail and severe wind are considered to be relatively high considering that nominal ~5x3 km spatial (at the domain center) and 15 min temporal resolution SEVIRI IRW data are used as input within the IRW-texture method. It is well known that OTs 1) often have a diameter of ≤ 15 km and can persist for < 15 mins (Shenk 1974; Bedka et al. 2010) and 2) do not always correspond with well-defined IRW BT minima, especially as image spatial resolution becomes coarse (Setvak et al. 2008, Bedka et al. 2010). Thus it is possible that an OT exists near a severe event but is not well observed by SEVIRI or it is not prominent enough for detection by the IRW-texture method. On the other hand, it is also possible that a well-defined OT need not be present for a storm to produce severe weather. Use of 5-min resolution rapid-scan SEVIRI data could improve the OT and severe weather relationship because there is a better chance of OT detection if given more frequent imagery. Rapid scan data is only available to the authors on a per-case basis, so we cannot adequately test this hypothesis.

5. Summary

This paper demonstrated an objective OT detection method using MSG SEVIRI IRW imagery and provided an OT database for all operational SEVIRI data over Europe and north Africa for six Northern Hemisphere warm seasons. Algorithm performance was demonstrated for 25 May 2009 when numerous severe storms were present.

Qualitative comparison indicated that most OT detections corresponded with the characteristic OT signature in visible channel imagery, but some OTs were left undetected. An example of a well-defined OT in the visible channel showed that cold SEVIRI IRW BTs were not co-located with this OT, thus inhibiting detection. Another well-documented OT detection technique based on the WV-IRW brightness temperature difference was shown for this storm. This technique was unable to clearly depict this OT and numerous other false detections were also evident in non-OT regions, demonstrating the challenges of objective OT detection with current-generation infrared channel data and existing techniques. Despite the evidence of missed detections, the results shown here combined with previous results of Bedka et al. (2010) indicate that the IRW-texture technique is suitable for producing a long-term MSG SEVIRI OT database.

The six warm season SEVIRI OT database showed a strong relationship with relative OT maxima and regions of high terrain. OTs were found to occur more frequently during the day over land than during the night and over water, similar to the results of Bedka et al. (2010) for the U.S. The number of daytime detections peaks sharply at 15 UTC near the time of maximum land surface temperature and greatest atmospheric instability. A bi-modal distribution of OTs is evident, with a broad maximum from 11 to 22 UTC and a secondary maximum from 04 to 07 UTC. Significantly fewer OTs were detected during the 2005 and 2006 seasons in association with drought conditions over Europe. A steady increase in OT detection has occurred each year from 2007 to 2009. Maximum OT occurrence is in May and June over continental Europe, and in September over the Mediterranean Sea. There were also interesting

intra-seasonal shifts in OT detections coincident with changes in the favored climatological locations for storm development throughout the warm season.

Confirmed severe wind, large hail, and tornado events from the ESWD were compared to OT detections to determine how often OTs are detected near the time and location of confirmed severe weather reports. An OT was found in the vicinity of severe weather events for 643 or ~44% of the 1475 confirmed reports. The relationship is strong for large hail (53%) and severe wind (52%) events but relatively weak for tornadoes (14%). Strong atmospheric instability (i.e. CAPE) is necessary to produce the intense updrafts required for OTs, but also large hail formation. Earlier studies had shown that large low-level wind shear values are found more often than high CAPE in tornadic thunderstorm environments across Europe. Weaker updrafts in tornadic storms relative to storms that produce severe hail/winds result in a less prominent or possibly non-existent OT signature in IRW BT imagery. Other studies had documented a weakening of the storm updraft and collapse of the OT region in advance of tornado formation. For tornado reports with a temporal confidence of +/- 15 mins, the results of this study show that less than 10% of OTs were found prior to the time of the tornado, supporting the OT collapse hypothesis. We hypothesize that these two factors contribute strongly to the weak OT-tornadic storm relationship, but acknowledge that this needs corroboration from a larger number of warm seasons with SEVIRI data.

MSG SEVIRI currently provides the best operational, geostationary-orbiting proxy for the future GOES-R ABI. The results of this study demonstrated that the IRW-texture method provides reliable OT detection results at latitudes comparable to the northern U.S. and southern Canada and would be suitable for future operational use with GOES-

R ABI. Future work will be directed toward quantifying the relationship between OTs and severe weather across the U.S. in addition to an objective validation of IRW-texture OT detections for both polar-orbiting and geostationary imagers using truth OT observations from the NASA A-Train constellation.

6. Acknowledgements

I thank Pieter Groenemeijer and Nikolai Dotzek (ESSL) for providing the ESWD data from www.eswd.eu. I also thank Pieter and Nikolai, Patrick Minnis (NASA LaRC), Martin Setvak (CHMI), Jason Brunner (UW-SSEC/CIMSS), and Richard Dworak (UW-SSEC/CIMSS) for valuable feedback. Lastly, I thank the UW-SSEC Data Center for providing access to the MSG SEVIRI data archive. This research was supported by the NASA Applied Sciences Advanced Satellite Aviation-Weather Products program.

7. References

Adler, R.F., and D.D. Fenn, 1981: Satellite-Observed Cloud-Top Height Changes in Tornadic Thunderstorms. *J. Appl. Meteor.*, **20**, 1369–1375.

Adler, R. F., M. J. Markus, D. D. Fen, G. Szejwach, and W. E. Shenk, 1983: Thunderstorm top structure observed by aircraft overflights with an infrared radiometer. *J. Appl. Meteor. And Climatol.*, **22**, 579-593.

Adler, R.F., M.J. Markus, and D.D. Fenn, 1985: Detection of severe Midwest thunderstorms using geosynchronous satellite data. *Mon. Wea. Rev.*, **113**, 769–781.

Amante, C., and B. W. Eakins, 2009: ETOPO1 1 Arc-minute global relief model:

Procedures, data sources, and analysis. NOAA Technical Memorandum NESDIS NGDC-24.

Bedka, K. M., Brunner J, Dworak R, Feltz W, Otkin J, et al., 2010: Objective Satellite-Based Overshooting Top Detection Using Infrared Window Channel Brightness Temperature Gradients. *J. Appl. Meteor. and Climatol.*, **49**, 181-202.

Bedka, K. M, and P. Minnis, 2010: GOES-12 observations of convective storm evolution and variability during the TC4 field program. In Press.

Bissolli, P., J. Grieser, N. Dotzek, and M. Welsch, 2007: Tornadoes in Germany 1950-2003 and their relation to particular weather conditions. *Global and Planetary Change*, **57**, 124-138..

Brooks, H. E., J. W. Lee, and J. P. Craven, 2003: The spatial distribution of severe thunderstorm and tornado environments from global reanalysis data. *Atmos. Res.*, **67-68**, 73-94.

Brooks, H. E., 2009: Proximity soundings for severe convection for Europe and the United States from reanalysis data. *Atmos. Res.,* **93**, 546-553.

Brunner J.C., S.A. Ackerman, A.S. Bachmeier, and R.M. Rabin, 2007: A quantitative analysis of the enhanced-V feature in relation to severe weather. *Wea. Forecasting*, **22**, 853–872.

Dotzek, N., 2001: Tornadoes in Germany. *Atmos. Res*., **56**, 233-251.

Dotzek, N., and K. Friedrich, 2009: Downburst-producing thunderstorms in southern Germany: Radar analysis and predictability. *Atmos. Res*., **93**(1-3), 457-473.

Dotzek, N., P. Groenemeijer, B. Feuerstein, and A. M. Holzer, 2009: Overview of ESSL's severe convective storms research using the European Severe Weather

Database ESWD. *Atmos. Res.*, **93**, 575-586.

Giaiotti, D. B., M. Giovannoni, A. Pucillo, F. Stel, 2007: The climatology of tornadoes and waterspouts in Italy. *Atmos. Res.*, **83**, 534-541

Groenemeijer, P., and co-authors, 2004: ESWD – A standardized, flexible data format for severe weather reports. *Preprints, 3rd European Conf. on Severe Storms*, León, Spain, 9-12 November 2004, 2 pp. [Available at www.essl.org/projects/ESWD/pdf/preprint.pdf]

Groenemeijer, P., T. Kühne, Z. Liang, and N. Dotzek, 2009: New capabilities of the European Severe Weather Database (ESWD), Preprints, 5th European Conf. on Severe Storms, Landshut, Germany, 12-16 October 2009, 2 pp. [Available at www.essl.org/ECSS/2009/preprints/O10-3-groenemeijer.pdf]

Groenemeijer, P., and A. van Delden, 2007: Sounding-derived parameters associated with large hail and tornadoes in the Netherlands. *Atmos. Res.*, **83**, 473-487

Horvath, A., and I. Geresdi, 2003: Severe storms and nowcasting in the Carpathian basin. *Atmos. Res.*, **67-68**. 319-332.

Kaltenböck, R., G. Diendorfer, and N. Dotzek, 2009: Evaluation of thunderstorm indices from ECMWF analyses, lightning data and severe storm reports. *Atmos. Res.*, **93**, 381-396.

Lemon, L.R., D.W. Burgess, and R.A. Brown, 1978: Tornadic Storm Airflow and Morphology Derived from Single-Doppler Radar Measurements. *Mon. Wea. Rev.*, **106**, 48–61.

Machado, L. A. T., W. F. A. Lima, O. Pinto, and C. A. Morales, 2009: Relationship between cloud-to-ground discharge and penetrative clouds: A multi-channel

satellite application. *Atmos. Res.*, **93**, 304-309.

Morel C. and S. Sénési, 2002: A climatology of mesoscale convective systems over Europe using satellite infrared imagery. II: Characteristics of European mesoscale convective systems. *Quarterly Journal of the Royal Meteorological Society*. ISSN 0035-9009.

Negri, A. J., and R. F. Adler, 1981: Relation of satellite-based thunderstorm intensity to radar-estimated rainfall. *J. Appl. Meteor.*, **20**, 288–300.

Reynolds, D.W., 1980: Observations of damaging hailstorms from geosynchronous satellite digital data. *Mon. Wea. Rev.*, **108**, 337–348.

Rivas Soriano, L. R., and F. de Pablo, 2002: Maritime cloud-to-ground lightning: The western Mediterranean Sea. *J. Geophys. Res.*, **107**, 4597.

Sanchez, J. L., M. V. Fernandez, J. T. Fernandez, E. Tuduri, and C. Ramis, 2003: Analysis of mesoscale convective systems with hail precipitation. *Atmos. Res.*, **67-68**, 573-588.

Sander, J., N. Dotzek, and R. Sausen, 2008: First results of climate change impacts on severe convective storms over Europe. *Preprints, 24th Conference on Severe Local Storms*, Savannah, 27-31 October 2008, Amer. Meteor. Soc., Boston, 4 pp. [Available at http://ams.confex.com/ams/24SLS/techprogram/paper_142105.htm]

Schmit, T.J., M.M. Gunshor, W.P. Menzel, J.J. Gurka, J. Li, and A.S. Bachmeier, 2005: Introducing the next-generation Advanced Baseline Imager on GOES-R. *Bull. Amer. Meteor. Soc.*, **86**, 1079–1096.

Schulz, W., K. Cummins, G. Diendorfer, M. Dorninger, 2005: Cloud-to-ground lightning in Austria: A 10-year study using data from a lightning location system. J. Geophys. Res., **110**.

Setvak, M., M. Salek, J. Munzar, 2003: Tornadoes within the Czech Republic: From early Medieval chronicles to the internet society. *Atmos. Res.*, **67-68**, 589-605.

Setvak, M., D. T. Lindsey, P. Novak, R. M. Rabin, P. K. Wang, M. Radova, J. Kerkmann, L. Grasso, S-H. Su, R. M. Rabin, J. Stastka, Z. Charvat, 2010: Satellite-observed cold-ring shaped features atop convective clouds. *Atmos. Res.*, **97**, 80-96.

Shenk, W. E., 1974: Cloud Top Height Variability of Strong Convective Cells. *J. Appl. Meteor.*, **13**, 917–922.

Sioutas, M. V.,2003: Tornadoes and waterspouts in Greece. *Atmos. Res.,* **67-68**, 645-656.

Steiger, S. M., R.E. Orville, and L.D. Carey, 2007: Total Lightning Signatures of Thunderstorm Intensity over North Texas. Part I: Supercells. *Mon. Wea. Rev.*, **135**, 3281–3302.

Tuovinen, J. P., A. J. Punkka, J. Rauhala, H. Hohti, D. M. Schultz, 2009: Climatology of severe hail in Finland: 1930-2006. *Mon. Wea. Rev.*, **137**, 2238-2249.

Webb, J. D. C., Elsom, D. M., and G. T. Meaden, 2009: Severe hailstorms in Britain and Ireland, a climatological survey and hazard assessment. *Atmos. Res.*, **93**, 587-606.

List of Figure Captions

Figure 1: A one arc-minute spatial resolution surface elevation map of the study domain from the National Oceanographic and Atmospheric Administration “ETOPO1” dataset.

Figure 2: Large hail, heavy rain, severe wind gust, and funnel cloud reports (n = 24) recorded in the European Severe Weather Database with QC-levels QC1 and QC2 between 1000 and 1659 UTC on 25 May 2009. Image courtesy of the European Severe Storms Laboratory.

Figure 3: Hourly MSG SEVIRI 10.8 μm channel brightness temperature imagery from a) 1000 UTC to h) 1700 UTC on 25 May 2009. Pixels with brightness temperature ≤ 225 K are shown.

Figure 4: Objective overshooting top detections from 1000 to 1645 UTC on 25 May 2009 using the IRW-texture method. The color of the square corresponds to the time of the overshooting top detection as specified in the legend.

Figure 5: A time series of 3 km MSG SEVIRI 10.8 μm brightness temperature (left column), 1 km MSG SEVIRI high resolution visible (HRV, middle column), and 1 km HRV imagery with objective OT detections (colored squares, right column) for deep convective storms over the English Channel. The time series begins at 1430 UTC on 25 May 2009 (top row) and continues at half-hourly intervals until 1600 UTC (bottom row). Only IRW BT ≤ 225 K are shown. The color of the OT detection boxes correspond to the legend of Figure 4. The arrows in the center column show the locations of an OT in storm A identified via subjective HRV image analysis.

Figure 6: a) 1 km MSG SEVIRI HRV, b) 3 km MSG SEVIRI 10.8 μm brightness temperature, and c) WV-IRW BTD imagery at 1530 UTC on 25 May 2009 over the same domain shown in Figure 5. Only IRW BT ≤ 225 K and positive WV-IRW BTD values are shown.

Figure 7: A time series of 3 km MSG SEVIRI 10.8 μm brightness temperature (left column), 1 km MSG SEVIRI high resolution visible (HRV, middle column), and 1 km HRV with objective overshooting top detections (colored squares, right column) for deep convective storms along the border between Austria and Slovenia. The time series begins at 1500 UTC on 25 May 2009 (top row) and continues at half-hourly intervals until 1630 UTC (bottom row). Only IRW BT ≤ 225 K are shown. The color of the OT detections correspond to the legend of Figure 4.

Figure 8: a) 1 km MSG SEVIRI HRV, b) 3 km MSG SEVIRI 10.8 μm brightness temperature, and c) WV-IRW BTD imagery at 1600 UTC on 25 May 2009 over the same domain shown in Figure 7. Only IRW BT ≤ 225 K and positive WV-IRW BTD values are shown.

Figure 9: IRW-texture overshooting top detections on a 0.50° grid. a) All overshooting top detections, b) daytime only (0900 AM to 0859 PM LST), c) night-time only (0900 PM

to 0859 AM LST), and d) the fraction of overshooting top detections occurring during the daytime. This fraction is computed over 1.5° x 1.5° grid boxes such that a significant OT sample size is used to determine this statistic. Warm (Cool) colors in panel d) indicate that more tops were detected during the day (night). Only locations with 5 or more OTs in a 1.5° grid box are shown.

Figure 10: The fraction of detected overshooting tops that occurred within a given hour, with the solid (dashed) line corresponding to detections over land (water).

Figure 11: OT detections during the 0500 to 0745 AM local time period from April-September 2004-2009.

Figure 12: Overshooting top detections separated by year with a) corresponding to 2004 and f) corresponding to 2009.

Figure 13: Overshooting top detections from 2004-2009 separated by month, with a) corresponding to April and f) corresponding to September.

Pixel Location	Line Sampling Distance	Element Sampling Distance
Southwest Corner 30° N, 10° W	3.8 km	3.1 km
Domain Center 45° N, 10° E	5.2 km	3.2 km
Northeast Corner 60° N, 30° E	10.6 km	4.4 km

Table 1: The pixel sampling distance in the line and element directions of MSG SEVIRI 10.8 μm channel pixels at the southwest corner, domain center, and northeast corner of the study domain.

Severe Weather Type	Number of Matching Overshooting Tops	Number of Severe Weather Occurrences	Match Percentage
Tornado	48	345	14%
Severe Wind	248	477	52%
Large Hail	347	653	53%
All Types	643	1475	44%

Table 2: The number of events where overshooting cloud tops were found to occur near to the locations of tornado, severe wind, and large hail events recorded within the European Severe Weather Database.

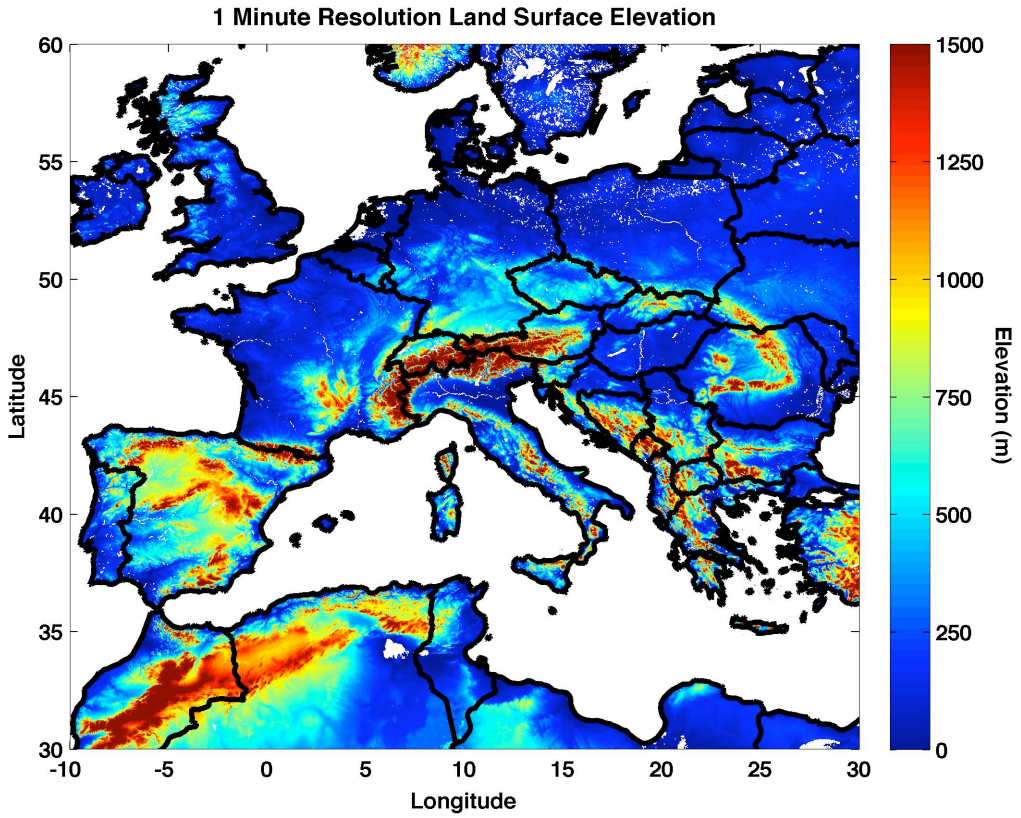

Figure 1: A one arc-minute spatial resolution surface elevation map of the study domain from the National Oceanographic and Atmospheric Administration “ETOPO1” dataset.

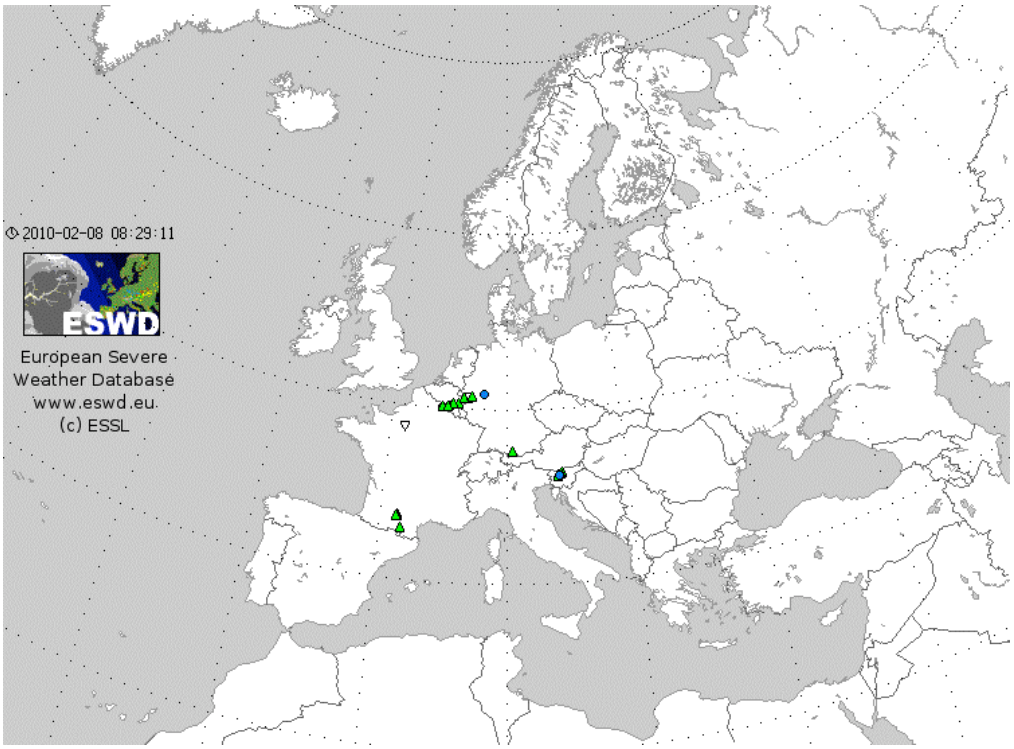

Figure 2: Large hail, heavy rain, severe wind gust, and funnel cloud reports (n = 24) recorded in the European Severe Weather Database with QC-levels QC1 and QC2 between 1000 and 1659 UTC on 25 May 2009. Image courtesy of the European Severe Storms Laboratory.

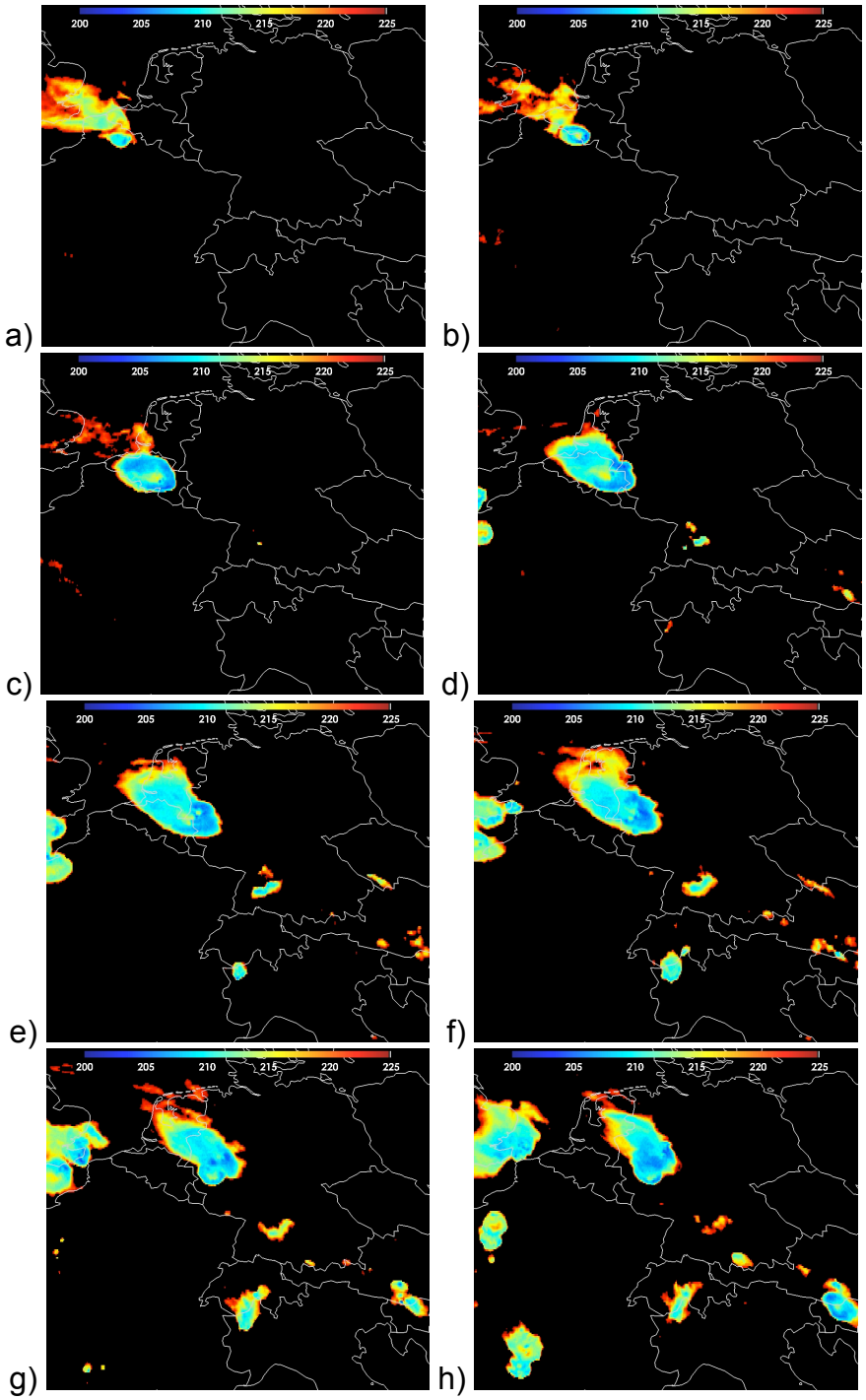

Figure 3: Hourly MSG SEVIRI 10.8 μm channel brightness temperature imagery from a) 1000 UTC to h) 1700 UTC on 25 May 2009. Pixels with brightness temperature ≤ 225 K are shown.

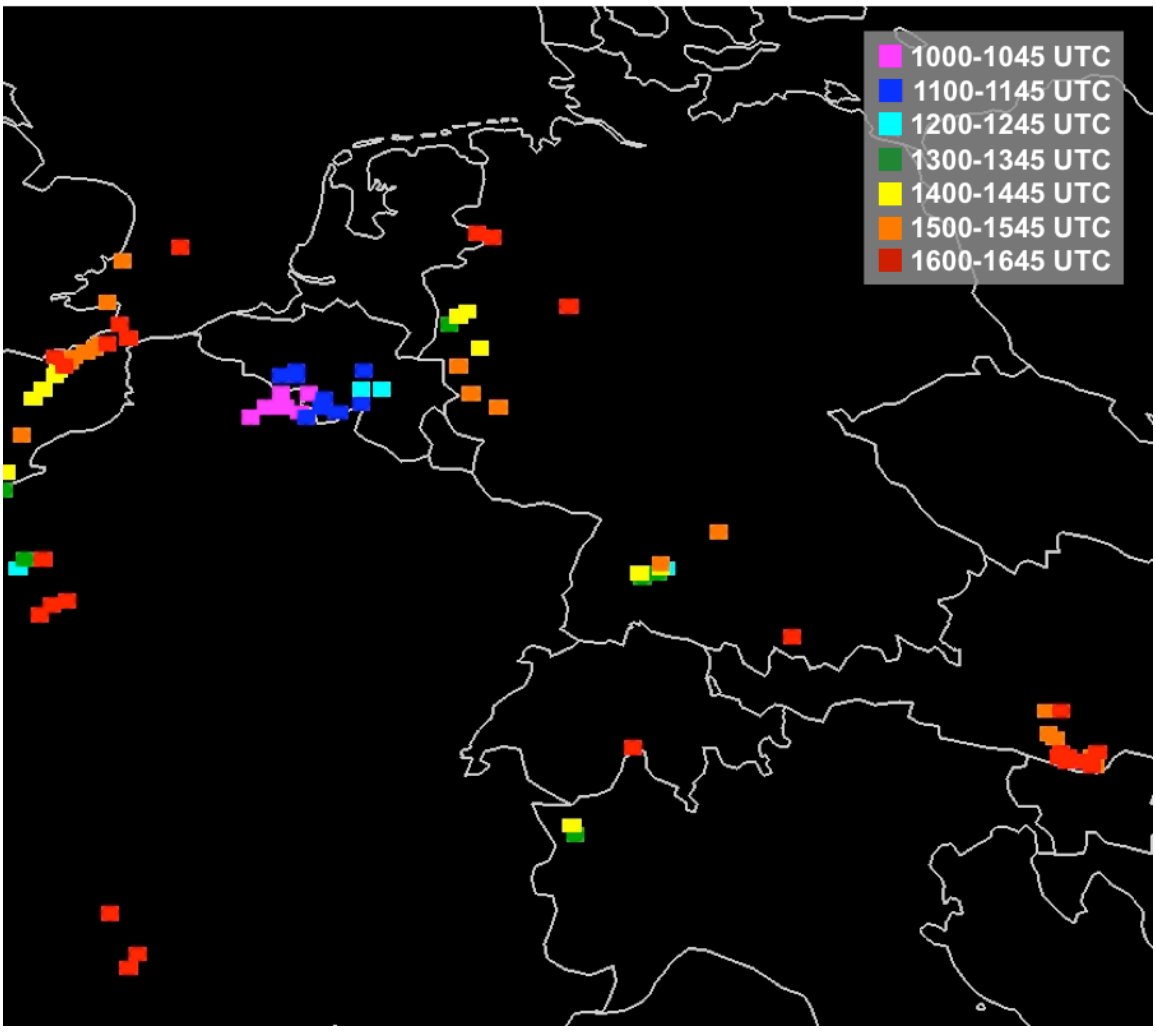

Figure 4: Objective overshooting top detections from 1000 to 1645 UTC on 25 May 2009 using the IRW-texture method. The color of the square corresponds to the time of the overshooting top detection as specified in the legend.

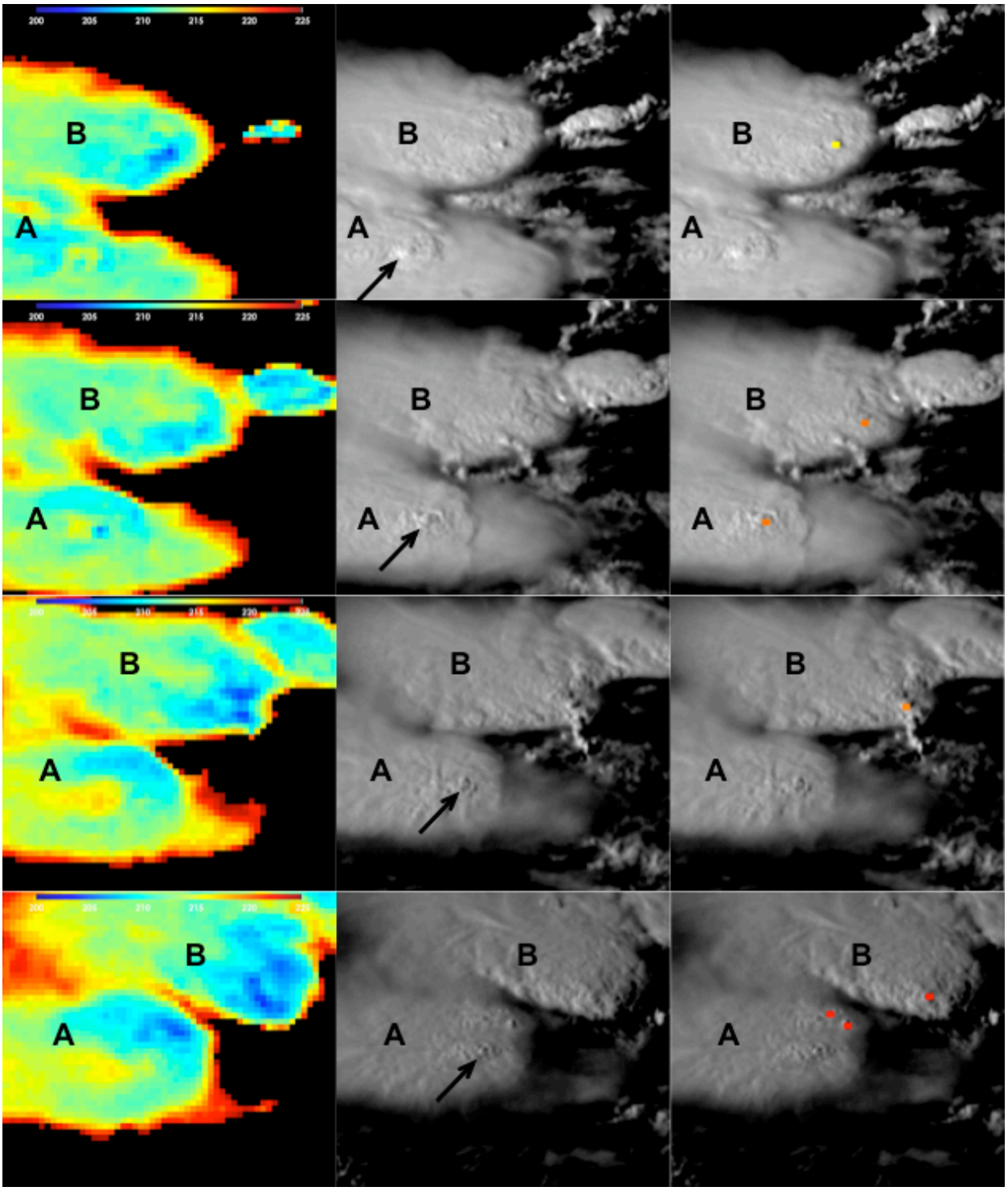

Figure 5: A time series of 3 km MSG SEVIRI 10.8 μm brightness temperature (left column), 1 km MSG SEVIRI high resolution visible (HRV, middle column), and 1 km HRV imagery with objective OT detections (colored squares, right column) for deep convective storms over the English Channel. The time series begins at 1430 UTC on 25 May 2009 (top row) and continues at half-hourly intervals until 1600 UTC (bottom row). Only IRW BT ≤ 225 K are shown. The color of the OT detection boxes correspond to the legend of Figure 4. The arrows in the center column show the

locations of an OT in storm A identified via subjective HRV image analysis.

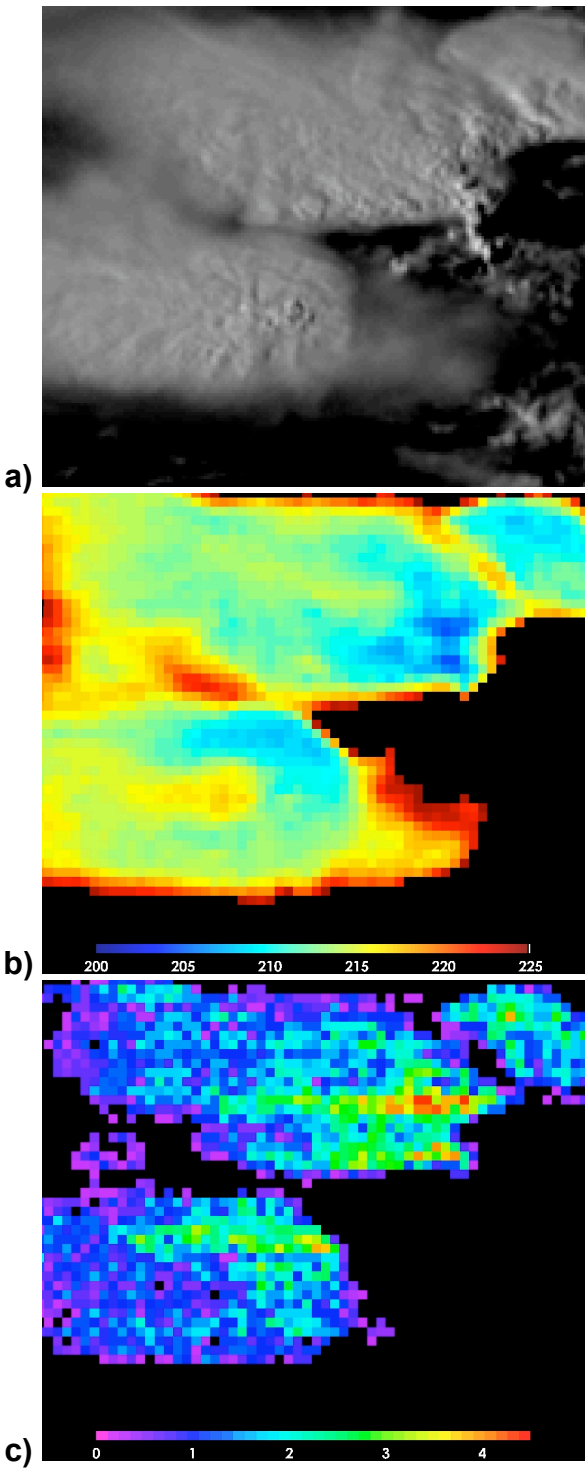

Figure 6: a) 1 km MSG SEVIRI HRV, b) 3 km MSG SEVIRI 10.8 μm brightness temperature, and c) WV-IRW BTD imagery at 1530 UTC on 25 May 2009 over the same domain shown in Figure 5. Only IRW BT ≤ 225 K and positive WV-IRW BTD values are shown.

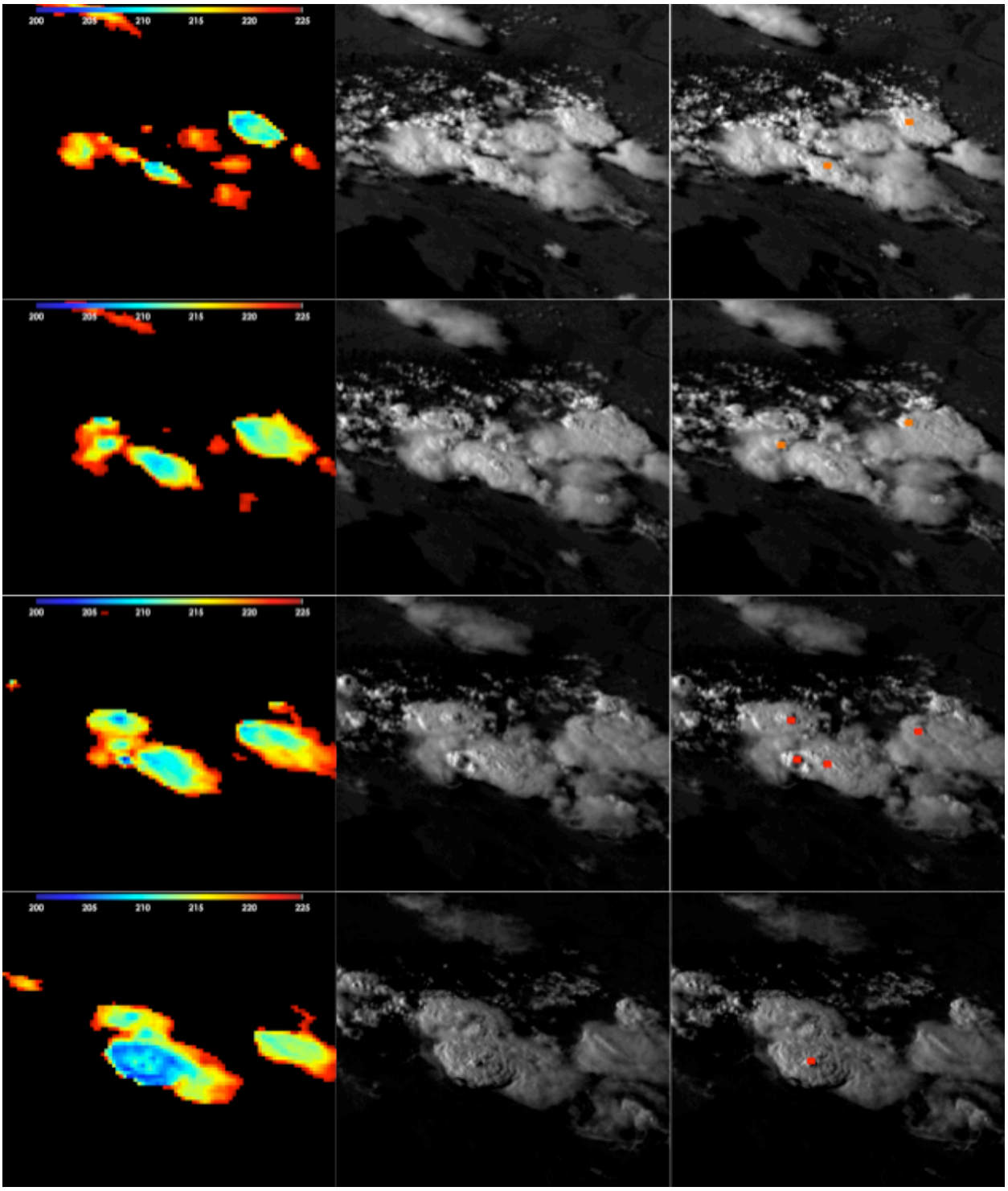

Figure 7: A time series of 3 km MSG SEVIRI 10.8 μm brightness temperature (left column), 1 km MSG SEVIRI high resolution visible (HRV, middle column), and 1 km HRV with objective overshooting top detections (colored squares, right column) for deep convective storms along the border between Austria and Slovenia. The time series begins at 1500 UTC on 25 May 2009 (top row) and continues at half-hourly intervals until 1630 UTC (bottom row). Only IRW BT ≤ 225 K are shown. The color of the OT detections correspond to the legend of Figure 4.

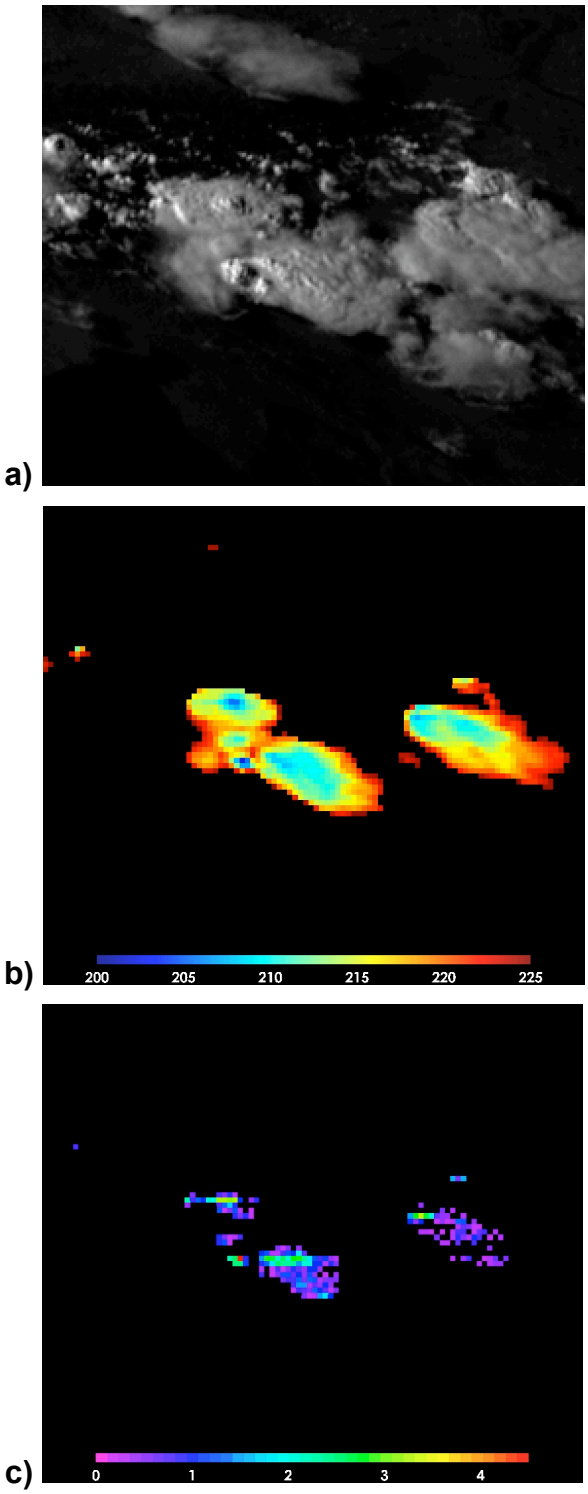

Figure 8: a) 1 km MSG SEVIRI HRV, b) 3 km MSG SEVIRI 10.8 μm brightness temperature, and c) WV-IRW BTD imagery at 1600 UTC on 25 May 2009 over the same domain shown in Figure 7. Only IRW BT ≤ 225 K and positive WV-IRW BTD values are shown.

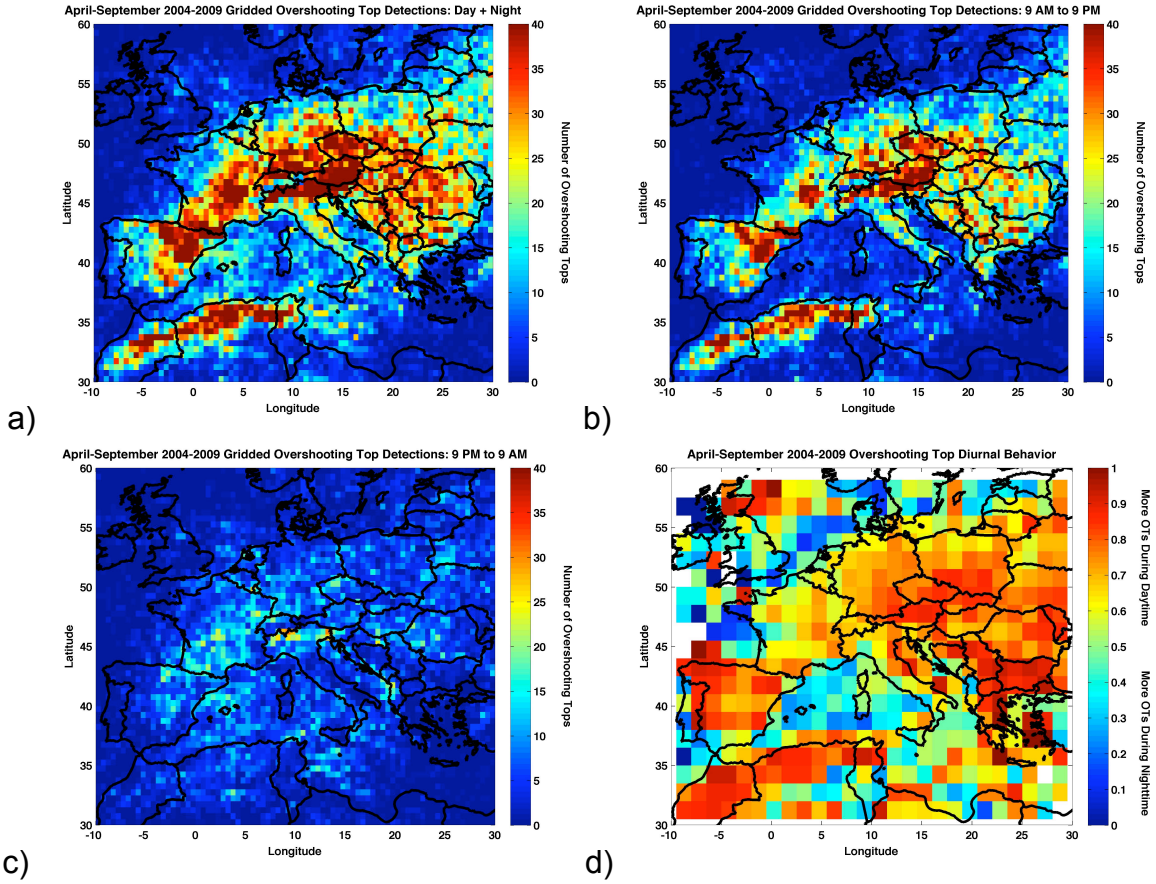

Figure 9: IRW-texture overshooting top detections on a 0.50° grid. a) All overshooting top detections, b) daytime only (0900 AM to 0859 PM LT), c) night-time only (0900 PM to 0859 AM LT), and d) the fraction of overshooting top detections occurring during the daytime. This fraction is computed over 1.5° x 1.5° grid boxes such that a significant OT sample size is used to determine this statistic. Warm (Cool) colors in panel d) indicate that more tops were detected during the day (night). Only locations with 5 or more OTs in a 1.5° grid box are shown.

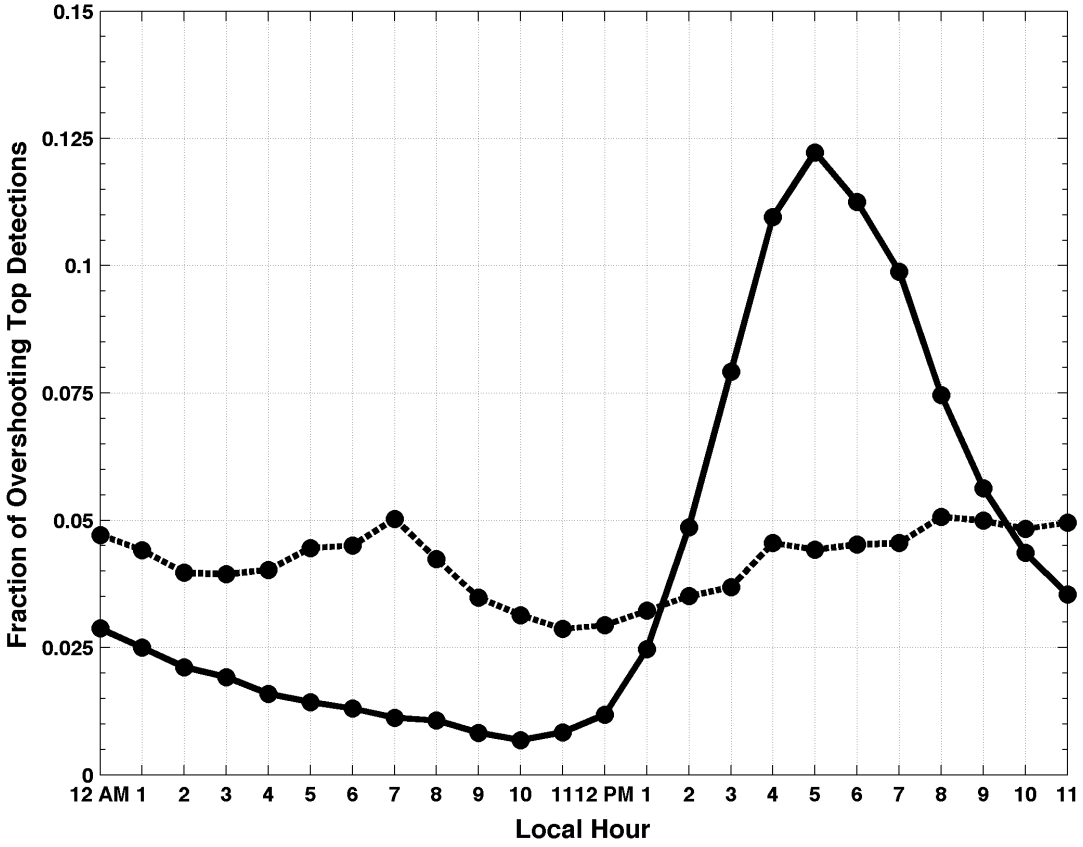

Figure 10: The fraction of detected overshooting tops that occurred within a given hour, with the solid (dashed) line corresponding to detections over land (water).

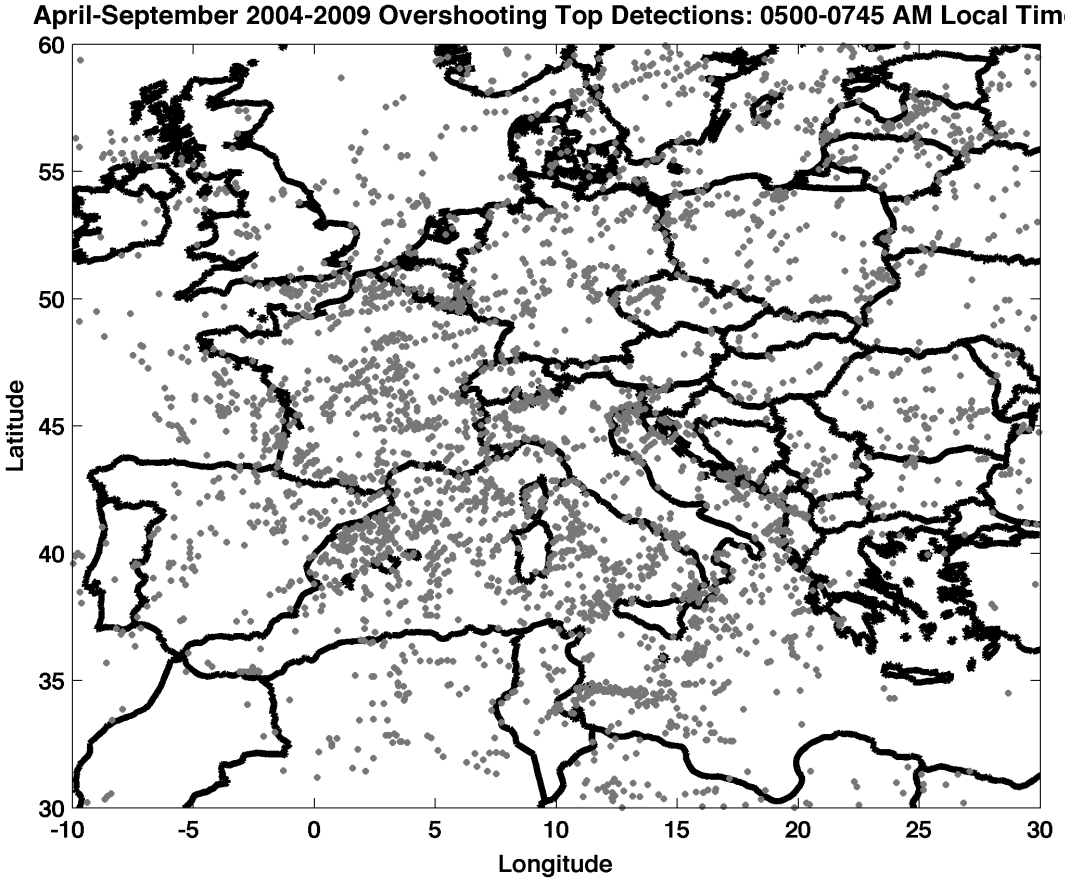

Figure 11: OT detections during the 0500 to 0745 AM LT period from April-September 2004-2009.

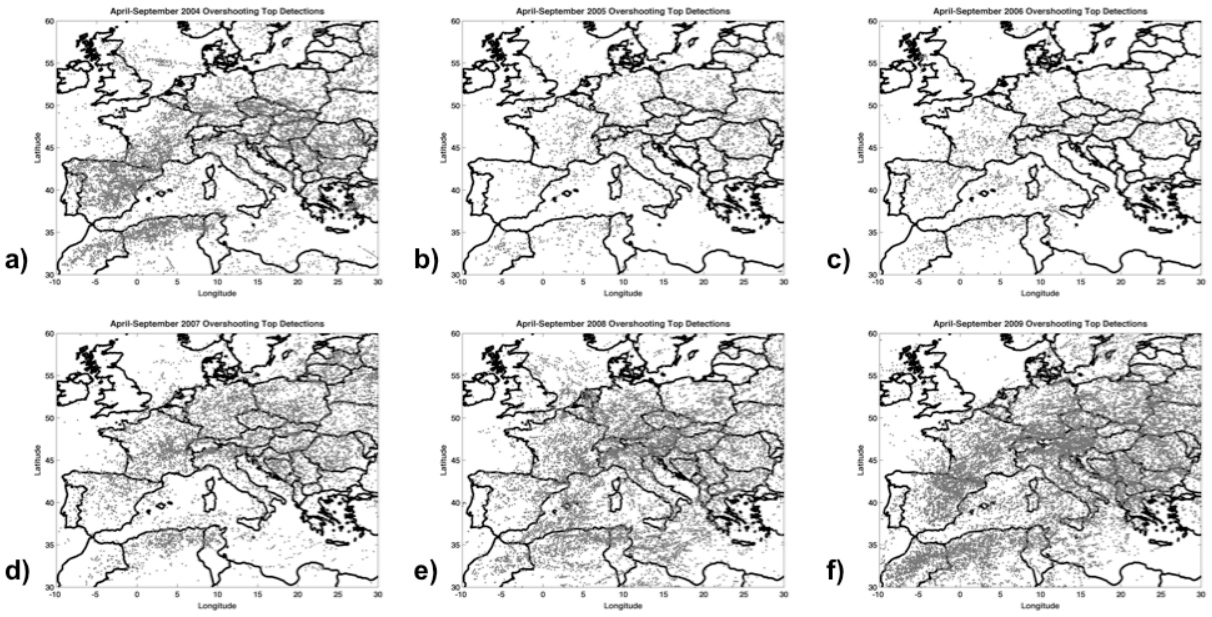

Figure 12: Overshooting top detections separated by year with a) corresponding to 2004 and f) corresponding to 2009.

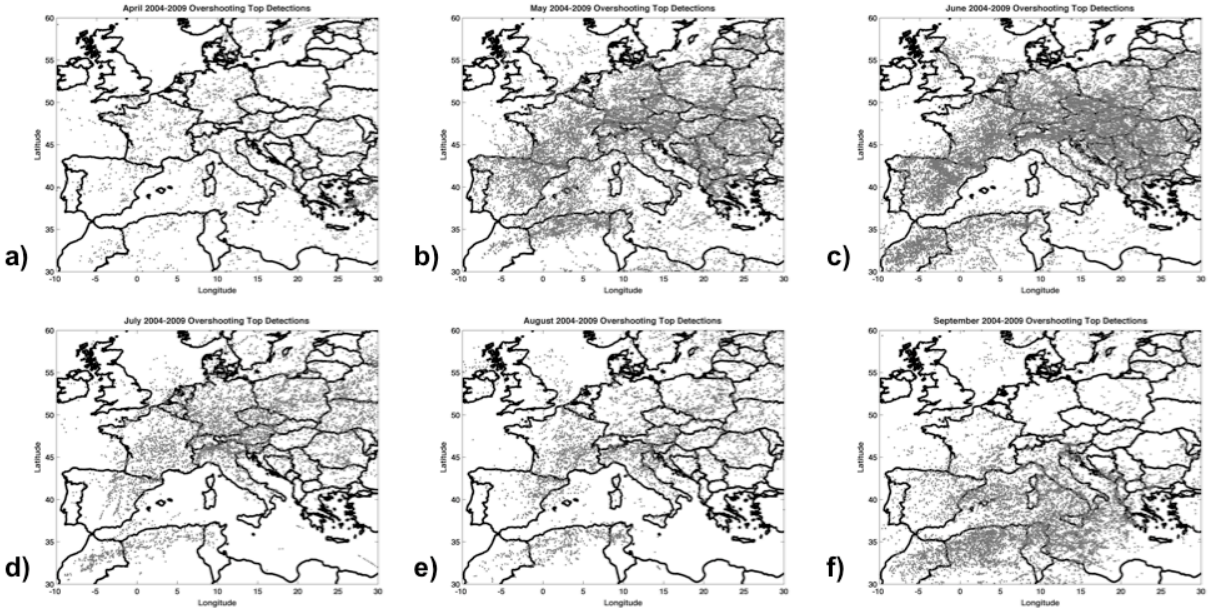

Figure 13: Overshooting top detections from 2004-2009 separated by month, with a) corresponding to April and f) corresponding to September.